Pis'ma v ZhETF, vol.68, iss.7, pp.572 - 577

NONLINEAR TRANSPORT THROUGH NS JUNCTIONS DUE TO IMPERFECT ANDREEV REFLECTION

G.B.Lesovik, G.Blatter[+]

Institute of Solid State Physics RAS, 142432 Chernogolovka, Moscow District, Russia

[+]*Theoretische Physik, ETH-Hönggerberg, CH-8093 Zürich, Switzerland*

Submitted 25 August 1998

We investigate a normal metal – superconductor (point) contact in the limit where the number of conducting channels in the metallic wire is reduced to few channels. As the effective Fermi energy drops below the gap energy, a conducting band with a width twice the Fermi energy is formed. Depending on the mode of operation, the conduction band can be further squeezed, leading to various non-linear effects in the current-voltage characteristics such as current saturation, a N-shaped negative differential resistance, bistability, and hysteresis.

PACS: 72.10.-d, 72.20.Ht, 74.50.+r, 74.80.Fp

Coherent transport phenomena in micro-structured normal–superconductor (NS) systems have recently attracted a lot of interest [1]. The transport across a NS boundary is governed by the phenomenon of Andreev reflection [2]: An electron incident from the normal metal on the NS junction with an excitation energy $|\varepsilon|$ below the superconducting gap Δ cannot penetrate into the bulk superconductor (we measure the excitation energy ε of the electron with respect to the chemical potential μ in the superconductor). Nevertheless, subgap transport across the junction is possible via the process of Andreev reflection, where the electron incident on the boundary is accompanied by a (coherent reflected) hole, producing effectively a state with two incoming electrons which convert into a Cooper pair upon entering the superconductor. For an ideal NS boundary, such a process leads to a conductance $G = 4e^2/h$ per channel [3], twice higher than the maximally possible normal one. If the transparency T of the boundary is smaller than unity, the NS linear conductance decreases as T^2 at small $T \ll 1$ [3]. New effects appear in the finite-bias or finite-temperature conductance when the transmission of electrons and holes differs significantly as a consequence of their different longitudinal kinetic energies [1, 4 – 6]. In this letter we show how Andreev scattering, combined with specific conditions for the propagation of electrons and holes, leads to the formation of a subgap conduction band with a width which strongly depends on the bias voltage, leading to new transport characteristics exhibiting a negative differential resistance, bistable, and hysteretic effects.

To fix ideas, consider a single channel normal metal point contact to a bulk superconductor, see Fig. 1(a). Here we have in mind geometries such as quantum point contacts realized in heterostructures [7, 8] or via manipulations with a scanning tunneling microscope [9]. Given the chemical potential μ, we define the longitudinal chemical potential $\mu_x = \mu - \varepsilon_\perp$, where $\varepsilon_\perp$ denotes the transverse energy of quantization in the normal channel. Here, we are interested in situations where the longitudinal kinetic energy $K_{e,h}$ at the Fermi surface is small, such that the condition $\mu_x < \Delta$ is realized. In this case, electrons with excitation energies $\varepsilon = E - \mu = K_e - \mu_x > 0$ can propagate through the contact, whereas the corresponding hole state with the same excitation energy can propagate only if its kinetic energy $K_h = \mu_x - \varepsilon$ remains positive, i.e., $\varepsilon < \mu_x$ (in this simplified discussion

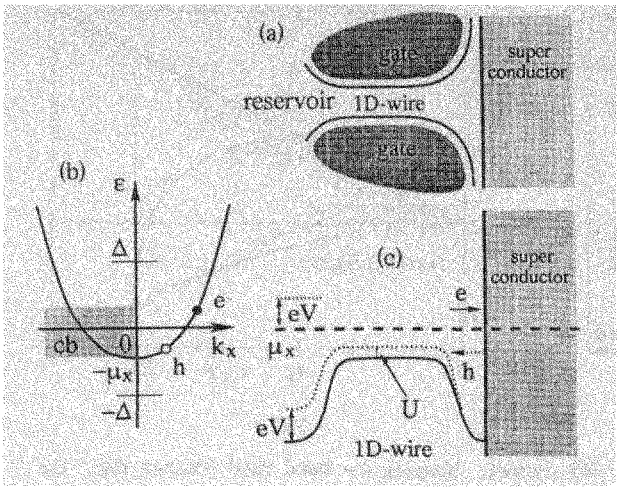

Fig.1. (a) Geometry of the NS point contact with the 1D normal wire adiabatically connected to the normal reservoir on the left and the bulk superconductor on the right, see Ref. [8]. (b) Dispersion relation in the normal wire. Note the formation of a conducting band (cb) of width $2\mu_x$. (c) Energy diagram for the wire sketched in (a). A change in bias eV induces a shift U in the wire potential, which in turn may lead to a reflection of the back-propagating hole. The electron then is normal-reflected from the NS boundary and does not contribute to the current

we assume that the conducting normal channel is long enough to generate transmission probabilities 0 or 1 only).

An electron incident on the superconductor defines the Andreev state (in the normal single channel region)

$$\Psi_\varepsilon(x) = \begin{pmatrix} 1 \\ 0 \end{pmatrix} \frac{e^{ik_+ x}}{\sqrt{v_+}} + \begin{pmatrix} r_{ee} \\ 0 \end{pmatrix} \frac{e^{-ik_+ x}}{\sqrt{v_+}} + \begin{pmatrix} 0 \\ r_{eh} \end{pmatrix} \frac{e^{ik_- x}}{\sqrt{v_-}}, \tag{1}$$

with $k_\pm = \sqrt{2m(\mu_x \pm \varepsilon)}/\hbar$ and $v_\pm = \hbar k_\pm/m$ (the above states are normalized to carry unit particle flux, with a normalization $\langle \Psi_\varepsilon, \Psi_{\varepsilon'} \rangle = 2\pi\hbar\delta(\varepsilon - \varepsilon')$, implying that $|r_{ee}|^2 = 1 - |r_{eh}|^2$). Following the above discussion, the quenching of the hole state for energies $\varepsilon > \mu_x$, combined with the restriction in the allowed energies for incident electron states $\varepsilon > -\mu_x$, leads to the formation of a conducting band of width $2\mu_x$, see Fig.1b and the inset of Fig.2. Within this band, incident electrons are (nearly) perfectly reflected into holes, whereas electrons with energies above this band ($\varepsilon > \mu_x$) are reflected as electrons and do not carry current (electrons with energies ($\varepsilon < -\mu_x$) do not enter the normal channel at all).

In the simplest formulation of the problem we consider a single channel NS junction. The Andreev states are found by solving the Bogoliubov – de Gennes equations

$$\begin{pmatrix} -\frac{\hbar^2\partial_x^2}{2m} - \mu_x & \Delta(x) \\ \Delta^*(x) & \frac{\hbar^2\partial_x^2}{2m} + \mu_x \end{pmatrix} \begin{pmatrix} u_\varepsilon(x) \\ v_\varepsilon(x) \end{pmatrix} = \varepsilon \begin{pmatrix} u_\varepsilon(x) \\ v_\varepsilon(x) \end{pmatrix} \tag{2}$$

with the gap function $\Delta(x) = \Delta\Theta(x)$, using the Ansatz (1) in the normal region and

$$\Psi_\varepsilon(x) = t_e \begin{pmatrix} 1 \\ \gamma \end{pmatrix} \frac{e^{(ip-q)x}}{\sqrt{v}} + t_h \begin{pmatrix} 1 \\ \gamma^* \end{pmatrix} \frac{e^{(-ip-q)x}}{\sqrt{v}} \tag{3}$$

in the superconducting region $x > 0$, with $p^2 - q^2 = 2m\mu_x/\hbar^2$, $pq = m\sqrt{\Delta^2 - \varepsilon^2}/\hbar^2$, $\gamma = (\varepsilon - i\sqrt{\Delta^2 - \varepsilon^2})/\Delta$, and the normalizing velocity $v = \hbar p/m$. Solving for the transmission and reflection coefficients we obtain the spectral conductance $G_{NS}(|\varepsilon| < \Delta) \approx \approx (8e^2/h)\Theta(\mu_x - |\varepsilon|)\sqrt{\mu_x^2 - \varepsilon^2}/\Delta$, valid in the limit $\mu_x \ll \Delta$ (see inset of Fig. 2; note that the Andreev approximation is not valid in the present case). Assuming a rigid band, implying that the applied bias drops at the boundary of the reservoir to the normal lead, the finite conduction band produces a current-voltage (I-V) characteristics $I = \int^{eV} d\varepsilon\, G_{NS}/e$

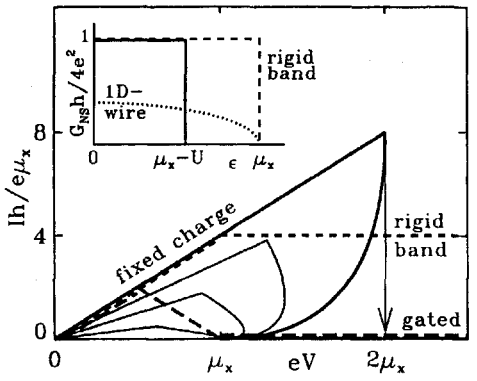

Рис.2

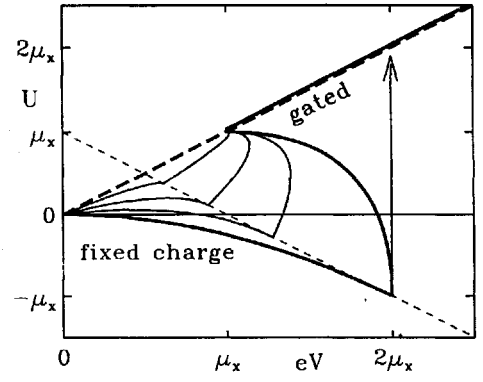

Рис.3

Fig.2. Current-voltage characteristics of the NS contact. Keeping the band rigid (dashed line), the current saturates when all electrons within the band $2\mu_x$ contribute. In the gated wire (long dashes), the back-propagation of holes is partially inhibited when the voltage increases beyond $\mu_x/2$ and completely quenched beyond $eV = \mu_x$. In the wire with fixed charge (thick solid line) the current switches from the upper to the lower branch, producing a pronounced negative differential resistivity. A finite reflectivity reduces the instability (fixed charge, thin solid lines, $|r_{ee}|^2 = 0.25,\ 0.5,\ 0.8$). Inset: Spectral conductance G_{NS} versus energy ϵ. For the 1D NS wire the conductance is suppressed due to imperfect Andreev reflection (dotted line). For the adiabatically connected wire of Fig.1a the Andreev approximation is applicable and G_{NS} reaches is maximal value. The width of the conduction band depends on the wire potential U (solid line: gated/fixed-charge wire; dashed line: rigid band)

Fig.3. Potential U within the normal wire versus applied bias for the case of a fixed charge and different values of the reflection coefficient r_{ee}, $r_{ee} = 0$ (thick solid line), $|r_{ee}|^2 = 0.25,\ 0.5,\ 0.8$ (thin solid lines). The lower branch becomes unstable at high applied bias and the internal potential U jumps to the gated value (long dashes), leading to a NDR in the I-V characteristics of the contact

which saturates at a bias $eV = \mu_x$ (we assume a negative bias $V < 0$, hence $eV > 0$). This then is the simplest example where the quenching of the back-propagating holes limits the width of the conducting band and entails a non-trivial saturation phenomenon in the transport characteristics of the NS junction. It is in contrast to the normal point contact, where an increasing bias eV opens up the channels, see Refs. [10] (note that a non-trivial structure in the I-V characteristics can occur in a normal point contact as well, though at much higher voltages $eV > \mu$, see [11]).

The above 1D example cannot be trivially applied to a physical situation: strictly speaking, we neither have a superconducting instability nor a normal Fermi liquid in a single channel 1D system. Let us then discuss the more realistic single channel NS point contact with a geometry as sketched in Fig.1a, see also [7]: The 1D normal wire is adiabatically connecting the normal reservoir with the bulk superconductor. The smooth form of the wire guarantees the appropriate matching of the wavefunctions in the three device segments, reservoir, 1D wire, and bulk superconductor. An imperfect matching leads to a normal reflection of the incident particle at the NS boundary and thus reduces the subgap transport with its interesting new features (below we will discuss the consequences of normal reflection for the device characteristics in more detail). The main properties of this geometry are the following: i) the confining potential of the wire produces a narrow conduction band connecting the reservoir with the NS boundary, ii) the 1D wire is long enough to guarantee a sharp onset of the transmission (but short enough to let us ignore strong interaction effects due to the one-dimensionality), iii) the wide NS contact helps

the proper matching of the wavefunctions, and iv) the large chemical potential in the bulk superconductor allows us to adopt the Andreev approximation. The functionality of this device resembles that of the idealized structure above: whereas in the 1D wire the back-propagation of the hole was limited by the bottom of the conduction band, in the present situation holes reflected from the NS boundary with minimal kinetic energy $\mu_x - \varepsilon < 0$ have to tunnel through the effective potential due to the transverse quantization in the wire, see Fig.1c.

As we can apply the Andreev approximation for the geometry of Fig.1a, the determination of the conductance is trivial, $G_{\rm NS}(\varepsilon) = (4e^2/h)\Theta(\mu_x - |\varepsilon|)$, and the corresponding I-V characteristics for the rigid band model follows from simple integration, see Fig.2.

So far, the determination of the current-voltage characteristics has been based on a rigid band model, where the voltage drop in the device occurs at the boundary to the normal reservoir. A more accurate calculation of the transport current $I(V)$ involves a self-consistent determination of the charge $\rho(x)$ and the electric potential $e\varphi(x)$ in the wire, given an applied bias V, see, e.g., Ref. [12]. Here we refrain from such a calculation, but rather discuss two interesting limiting cases illustrating the potential features of such a device.

The first case we wish to analyze is the gated wire, where a top gate placed over the wire modifies its potential $e\delta\varphi \equiv U(V, V_g)$. In the simplest case, considered by Brown *et al.* [11], the gate potential V_g follows the applied bias, $\delta V_g = V$. Assuming further that the wire potential is slaved to the gate, the band bottom in the wire is lifted by $U = eV$, implying that backpropagating holes and low energy incident electrons are cutoff at $|\varepsilon| = \pm(\mu_x - eV)$ rather than $\pm\mu_x$. Within the Andreev approximation the spectral conductance $G_{\rm NS}$ is narrowed down to the interval $|\varepsilon| < \mu_x - eV$ and takes the form

$$G_{\rm NS}(\varepsilon, U(V)) = \frac{4e^2}{h}\Theta[(\mu_x - U(V)) - |\varepsilon|]. \tag{4}$$

A simple integration produces the I-V characteristics

$$I(V < \Delta/e) = \frac{1}{e}\int_0^{eV} d\varepsilon G_{\rm NS}(\varepsilon, U(V)) \tag{5}$$

exhibiting a negative differential resistance (NDR) regime within the bias interval $\mu_x/2 < < eV < \mu_x$, see Fig. 2: Increasing the applied biased eV up to $\mu_x/2$, additional current carrying states are occupied and the transport current I increases. Going beyond the value $\mu_x/2$, the rising bottom of the band quenches the back propagation of the holes and fewer states are available, until at $eV = \mu_x$ all current carrying states are blocked.

The above NDR phenomenon is further accentuated in a device where the charge of the wire rather than its potential is fixed — this is the second limiting case we wish to study here. The contribution to the charge density of an individual channel averaged over the wire cross section is given by

$$\rho(x) = 2e\sum_k \{f_v(\varepsilon_k)|u_k(x)|^2 + [1 - f_v(\varepsilon_k)]|v_k(x)|^2\}, \tag{6}$$

with $f_v(\varepsilon)$ the (bias dependent) distribution function for the Bogoliubov quasi-particles. We evaluate the density in the middle of the wire and allow for a non-zero potential shift U. Using the normalization introduced in (1) we arrive at the form

$$\rho = \frac{e}{\pi\hbar}\int d\varepsilon \left[\frac{1 + |r_{ee}|^2}{v_+(\varepsilon)} f_v(\varepsilon) + \frac{|r_{eh}|^2}{v_-(\varepsilon)}[1 - f_v(\varepsilon)]\right], \tag{7}$$

with $v_\pm = \sqrt{2(\mu_x - U \pm \varepsilon)/m}$ the velocities of the quasiparticles. For the case of perfect Andreev reflection the above expression simplifies to [we assume an open channel configuration with $0 < eV < \mu_x - U$; the occupation numbers are determined by those of the metallic reservoir, $f_{\rm V}(\varepsilon) = \Theta(-\varepsilon + eV)$ at zero temperature]

$$\rho = \frac{e}{\pi\hbar}\sqrt{\frac{m}{2}}\left(\int_{-\mu_s+U}^{eV} d\varepsilon \frac{1}{\sqrt{\mu_x - U + \varepsilon}} + \int_{eV}^{\mu_s - U} d\varepsilon \frac{1}{\sqrt{\mu_x - U - \varepsilon}}\right). \tag{8}$$

Requiring that the charge difference $\delta\rho = \rho(eV, U) - \rho(0, 0)$ vanishes at any applied bias V leads to the condition ($k_{{\rm F},x} = \sqrt{2m\mu_x}/\hbar$)

$$\delta\rho = \frac{ek_{{\rm F},x}}{\pi}\left[\sqrt{1 - \frac{U - eV}{\mu_x}} + \sqrt{1 - \frac{U + eV}{\mu_x}} - 2\right] = 0,$$

determining the potential shift $U(V)$ in the wire. Solving for U we obtain the result

$$U(V) = -\frac{(eV)^2}{4\mu_x}, \quad 0 < eV < \mu_x - U(V). \tag{9}$$

The negative shift in the wire potential seems quite puzzling at first sight, but can be easily understood in terms of the reduced group velocity of the back-propagating holes. A second solution is found for a positive shift $U > \mu_x$, where the Andreev scattering is quenched and all incident electrons are reflected back as electrons ($|r_{ee}|^2 = 1$). With $\delta\rho = (2ek_{{\rm F},x}/\pi)[\sqrt{1 - (U - eV)/\mu_x} - 1] = 0$ we find the shift

$$U(V) = eV, \quad \mu_x - U(V) < 0 < eV. \tag{10}$$

Finally, a regime with partially quenched Andreev scattering is found in the interval $0 < \mu_x - U < eV$, with $U(V)$ determined by the relation $\delta\rho = (ek_{{\rm F},x}/\pi)$ $[2\sqrt{1 - (U - eV)/\mu_x} - \sqrt{2(1 - U/\mu_x)} - 2] = 0$ and the result

$$U = 2eV - 5\mu_x + 4\sqrt{\mu_x(2\mu_x - eV)}. \tag{11}$$

The internal potential shift U versus applied bias V is shown in Fig.3 (thick solid line). The three branches of $U(V)$ exhibiting completely open, partially quenched, and entirely quenched hole propagation in the wire arrange to define a typical bistable configuration of the wire within the bias interval $\mu_x < eV < 2\mu_x$. The lower branch with the open channel terminates at $eV = 2\mu_x$ and the system has to jump to the state where the backpropagation of holes is quenched. Physically, the jump between the two branches corresponds to a rearrangement of the potential drop in the device: At small bias (lower branch) the applied bias drops on the left side of the channel, towards the reservoir. At high bias (upper branch) the potential drops on the superconductor side, producing the gated situation described above. Translating this behavior of the internal device bias U to the I-V characteristics, see Fig.2, we find a jump from the 'open' current carrying state at low bias to the 'closed' gated state at high bias as the applied bias eV grows beyond the band width $2\mu_x$, thereby producing a characteristics with a N-shaped negative differential resistance. At voltages $eV > \Delta$ a finite conductance is restored. Note that the I-V characteristics is not symmetric: for a positive applied bias $V > 0$ ($eV < 0$) the conduction band stays open up to the bias $eV = -2\mu_x$, where the wire potential aligns with the potential in the reservoir, $U - \mu_x = eV$, see (9). Increasing the bias further, the current saturates (similarly to the rigid band case) as part of the incoming electrons are excluded from entering the wire.

The above analysis for the case of ideal Andreev reflection at the NS boundary can be easily generalized to take a finite normal reflectivity of the barrier into account. It is convenient to characterize the junction through its normal state properties: Given the reflection coefficient R for electrons entering the 1D wire, the parameter $|r_{ee}|^2$ switches between the values $|r_{ee}|^2 = 4R/(1+R)^2$ ('open' channel) and $|r_{ee}|^2 = 0$ ('closed' channel) (see Refs. [13, 6]; we assume that $\partial_\varepsilon R(\varepsilon) \approx 0$ and $\varepsilon \ll \Delta$, allowing us to ignore the energy dependence in $|r_{ee}|^2$). A finite value of R then leads to a smoothing of the potential-bias relation and the current-voltage characteristics, see Figs. 2 and 3. As R approaches unity the fixed-charge characteristics approaches the result of the gated wire.

Above we have concentrated on the single channel limit, where the non-linear effects leading to the NDR phenomenon are most pronounced. Going over to a multi-channel geometry, our analysis can be carried over to the grazing incidence trajectories [4] with the modification $\mu_x \to \mu_{x,n} = \mu - \varepsilon_{\perp,n}$, where $\varepsilon_{\perp,n} = \hbar^2 K_n^2/2m$ is the transverse energy of the n-th channel. The interesting structure obtained in the single channel case (see Fig. 2) then survives for the states with an effective chemical potential $\mu_{x,n} < \Delta$. The maximal number of channels to be saturated or cut off in this fashion below a bias $eV \sim \Delta$ is of order $\delta n \sim (\Delta/\mu)n$, where $n \gg 1$ is the total number of channels. In a bulk system with a planar NS boundary these states correspond to grazing incidence trajectories with angles $\vartheta < \sqrt{\Delta/\mu}$.

In conclusion, the different propagation conditions for electrons and holes in NS junctions produce a rich variety of phenomena. Both, the zero- and finite-bias anomalies [1] in dirty NS junctions can be understood in such terms [6]. Here, we have shown how the coherent electron-hole transport in a one/few channel system may lead to strong non-linearities in the device characteristics, resulting in an N-shaped NDR I-V curve in its most extreme variant. In conventional semiconductor devices this kind of instability leads to the formation of domain walls, e.g., the Gunn effect. In the present case where the transport is non-local and coherent we can expect a device operation more similar to that of a double-barrier resonant-tunneling structure [14].

We thank A.Fauchère, Ch.Glattli, I.Larkin, and L.Levitov for stimulating discussions and the Swiss National Foundation for financial support.

---

1. B.van Wees and H.Takayanagi, in: *Mesoscopic Electron Transport*, Eds. L.Son et al., NATO ASI Series Vol. 345, Kluwer, 1997, p.469, and references therein; C.W.J.Beenakker, in: *Mesoscopic Quantum Physics*, Eds. E.Akkermans et al., Elsevier, 1995.
2. A.F.Andreev, Sov. Phys. JETP **19**, 1228 (1964) [Zh. Eksp. Teor. Fiz. **46**, 1823 (1964)].
3. G.Blonder, M.Tinkham, and T.M.Klapwijk, Phys. Rev. **B25**, 4515 (1982).
4. Yu.K.Dzhikaev, Sov. Phys. JETP **41**, 144 (1975) [Zh. Eksp. Teor. Fiz. **68**, 295 (1975)].
5. G.Wendin and V.S.Shumeiko, Phys. Rev. **B53**, R6006 (1996).
6. G.B.Lesovik, A.L.Fauchére, and G.Blatter, Phys. Rev. **B55**, 3146 (1997).
7. H.Takayanagi, T.Akazaki, and J.Nitta, Phys. Rev. Lett. **75**, 3533 (1995).
8. D.A.Wharam et al., J. Phys. **C21**, L209 (1988); B.J.van Wees et al., Phys. Rev. Lett. **60**, 848 (1988).
9. A.P.Sutton, Curr. Opin. Solid State Mater. Sci. **1**, 827 (1996).
10. L.I.Glazman and A.V.Khaetskii, Europhys. Lett. **9**, 263 (1989); N.K.Patel et al., J. Phys. **C2**, 7247 (1990).
11. R.J.Brown et al., J. Phys. **C1**, 6285 (1989).
12. I.Larkin and J.Davies, Phys. Rev. **B52**, R5535 (1995).
13. C.W.J.Beenakker, Phys. Rev. **B46**, 12841 (1992).
14. V.J.Goldman, D.C.Tsui, and J.E.Cunningham, Phys. Rev. Lett. **58**, 1256 (1987).